Fluorine atom abstraction by Si(100) II. Model

M. R. Tate, D. P. Pullman,[a] Y. L. Li, D. Gosalvez-Blanco, A. A. Tsekouras,[b] and S. T. Ceyer[c]
Department of Chemistry, Massachusetts Institute of Technology, Cambridge, Massachusetts 02139

(Received 7 July 1999; accepted 20 December 1999)

A model is developed to describe the kinetics of the three scattering channels—unreactive scattering and dissociative chemisorption via single atom abstraction and two atom adsorption—that are present in the interaction of F_2 with Si(100). The model provides a good description of the non-Langmuirian coverage dependence of the probabilities of single atom abstraction and two atom adsorption, yielding insight into the dynamics of the gas–surface interaction. The statistical model is based on the premise that the two dissociative chemisorption channels share a common initial step, F atom abstraction. The subsequent interaction, if any, of the complementary F atom with the surface determines if the overall result is single atom abstraction or two atom adsorption. The results are consistent with the orientation of the incident F_2 molecular axis with respect to the surface affecting the probability of single atom abstraction relative to two atom adsorption. A perpendicular approach favors single atom abstraction because the complementary F atom cannot interact with the surface, whereas a parallel approach allows the F atom to interact with the surface and adsorb. The fate of the complementary F atom is dependent on the occupancy of the site with which it interacts. The model distinguishes between four types of dangling bond sites on the Si(100)(2×1) surface, based on the occupancy of the site itself and that of the complementary Si atom in the Si surface dimer. The results show that the unoccupied dangling bond sites on half-filled dimers are about twice as reactive as those on empty dimers, which is consistent with an enhanced reactivity due to a loss of a stabilizing π interaction between the two unoccupied dangling bonds on a dimer. [S0021-9606(00)70811-7]

I. INTRODUCTION

Recently, the absolute probabilities of all scattering channels in the interaction of F_2 with Si(100) have been measured as a function of fluorine coverage.[1] These reaction probabilities display an unexpected, non-Langmuirian dependence on coverage that arises not from adsorbate–adsorbate effects, which are the usual source of deviations from Langmuir kinetics, but from a nontraditional mechanism for dissociative chemisorption called atom abstraction.[2,3] In the classic mechanism, cleavage of the bond between the two atoms of a molecule incident on a surface is concomitant with the formation of a bond between each of the atoms and the surface. These two events must occur simultaneously because the energy released in the formation of two surface bonds is necessary to compensate for the energy required to cleave the molecular bond. In contrast, cleavage of the F_2 molecular bond upon formation of only a single bond to the Si surface is possible in atom abstraction because the F_2 bond energy is less than the energy released upon formation of the single Si–F bond. The complementary F atom may then scatter into the gas phase, a reaction channel termed single atom abstraction. Alternatively, it may then interact with the Si surface and possibly adsorb, even on a nonadjacent site, if it is scattered with the appropriate trajectory during the initial atom abstraction. This latter reaction channel is termed two atom adsorption. Although two atom adsorption results in the formation of two surface-adsorbate bonds just as in classic dissociative chemisorption, it is distinct from classic dissociative chemisorption in that it is not necessarily a concerted process mandated by the thermodynamics of the system, but rather is a stepwise process.

In the first of a series of papers on the interaction of F_2 with Si(100),[1] the absolute probability for F_2 to undergo either single atom abstraction or two atom adsorption on Si(100) was determined as a function of F_2 exposure by measuring the scattered F_2 and F atom flux. With the knowledge of the absolute incident molecular beam flux, the absolute probability for F_2 to access one of the two dissociative chemisorption channels was determined as a function of fluorine coverage. Figure 1 shows the probability of each of the scattering channels as a function of fluorine coverage. At low coverage, the dominant reactive channel is two atom adsorption, which has a probability, P_2, of 0.83 ± 0.03 in the limit of zero coverage. Despite being a seemingly second-order adsorption process, P_2 decreases almost linearly with coverage, deviating from linearity only near the saturation coverage of one monolayer (1 ML, one F atom per surface Si atom). Single atom abstraction is the minor channel at low coverage. Its probability, P_1, is 0.13 ± 0.03 in the limit of

[a]Permanent address: Department of Chemistry, San Diego State University.
[b]Permanent address: Department of Chemistry, University of Athens.
[c]Electronic mail: stceyer@mit.edu

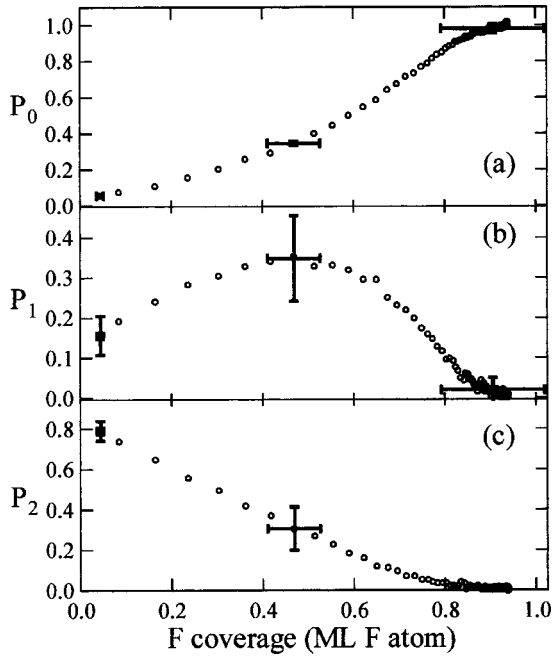

FIG. 1. Reaction probability of F_2 at $E_i = 0.7$ kcal/mol with Si(100) at 250 K as a function of fluorine coverage for (a) unreactive scattering P_0, (b) single atom abstraction P_1, and (c) two atom adsorption P_2. Data shown are average of six data sets interpolated to a common exposure interval and range. Error bars are propagated uncertainties typical of a single data set.

zero coverage and also exhibits a non-Langmuirian dependence on coverage, actually increasing to a maximum value of 0.35 ± 0.08 as the number of filled sites increases to 0.5 ML. At the maximum, P_1 and P_2 are nearly equal. As the coverage increases beyond 0.5 ML, P_1 and P_2 monotonically decay to zero around 1 ML.

In this second of a series of papers on the interaction of F_2 with Si(100), a simple yet physically intuitive statistical model is developed to describe the experimentally observed kinetics of the interaction of low energy F_2 with Si(100). The model describes the probability of single atom abstraction and two atom adsorption both as a function of exposure to F_2 and as a function of fluorine coverage, the relevant kinetic parameter. The model is based on the premise that two atom adsorption is not a concerted process, like classic dissociative chemisorption, and is intimately related to single atom abstraction. Specifically, the two dissociative chemisorption channels share a common initial step, F atom abstraction from the incident F_2 molecule by the Si(100) surface. The fate of the complementary F atom determines whether the overall result is single atom abstraction or two atom adsorption.

The model is also based on the premise that the reactivities of the different types of unoccupied sites on the Si(100) surface are not equivalent, a premise easily rationalized by the structure and bonding of the surface atoms in this covalent solid. Si(100) reconstructs forming rows of surface Si dimers, yielding a (2×1) periodicity that is observable by He and electron diffraction, and leaving one partially filled molecular orbital or dangling bond projecting into the vacuum for each surface Si atom. The remaining dangling bonds on each of the two Si atoms that comprise the dimer interact to form a weak π bond. The weakness of the π bond effectively leaves the dangling bonds as radical sites, which hence are very reactive and are the sites for F atom abstraction and adsorption as shown experimentally.[1] Nevertheless, when a F atom is adsorbed on one of the dangling bonds creating an occupied site, the weak π bond is broken, leaving the dangling bond of the complementary Si atom in a half-filled dimer more radical like and hence more reactive than dangling bonds of an empty dimer which are involved in a π interaction. Hence, the different reactivities of the two types of dangling bonds are based on the occupancy of the dangling bond on the complementary Si atom in the dimer.

The results of the theoretical model for P_1 and P_2, as well as for P_0, which is the probability of unreactive scattering, match the experimental measurements well. Most importantly, the model correctly predicts two distinct features of the experimental results: (1) The nonmonotonic dependence on the coverage of the probability of single atom abstraction and (2) the linear dependence on the coverage of the probability of two atom adsorption. Both features are unexpected from the traditional Langmuirian viewpoint of gas–surface chemical kinetics that predicts a power law dependence on the number of empty sites where the exponent is equal to the number of adsorbates that are created in the process. In other words, the probability of single atom abstraction is expected to be linear while the probability of two atom adsorption ought to be quadratic with respect to the number of unoccupied sites. The good agreement between the model and the data also provides further support for two atom adsorption as a stepwise dissociative chemisorption mechanism.

In addition to correctly predicting the experimentally measured kinetics of the gas–surface chemical reaction, the model also provides insight into the dynamics of the interaction. Scattering cross sections for the elementary steps of the interaction of both the F_2 molecule and the F atom with the different types of sites on the Si(100) surface are determined. The two types of unoccupied sites, those that are members of empty dimers and those that are members of half-filled dimers, display a substantially different reactivity towards fluorine. The allowance for different reactivities of the two types of unoccupied sites is shown to be critical for good agreement between the model and the data. The results also suggest that the orientation of the incident F_2 molecule relative to the surface plane determines the fate of the complementary F atom which must interact with the surface in order for two atom adsorption to occur.

The paper is divided into several sections. Section II gives a brief overview of the experimental results showing the determination of the absolute probabilities of the three reaction channels as a function of F_2 exposure and fluorine coverage. In Sec. III, the statistical model is developed from a minimal set of assumptions and compared to the experimental results. Section IV is a discussion of the model and its implications on the dynamics of the interaction between

F_2 and Si(100) as well as its limitations in describing a complex chemical interaction in simple statistical terms. The results from the experimental measurements and the theoretical model are compared with the results of previous experimental and theoretical work.

II. REVIEW OF EXPERIMENTAL RESULTS

The apparatus has been described in detail previously.[1,4] The results shown in Fig. 1 are derived from experimental data[1,5–7] in which a F_2 beam, with an average translational energy of $E_i = 0.7$ kcal/mol, is incident along the normal of the (100) plane of a Si crystal at 250 K. The scattered products are detected and identified by a triply differentially pumped, rotatable quadrupole mass spectrometer and their velocity distribution and flux are measured using a time-of-flight technique.

The coverage dependence of the three scattering channels is contained in the measurements of the flux of scattered F and F_2, the products of single atom abstraction and unreactive scattering, respectively, as a function of F_2 exposure. The probability is equal to the flux of scattered products relative to the incident F_2 flux, which is proportional to the scattered flux of F_2 at long exposures where the reaction with Si has ceased. The simplified equations for the probability of single atom abstraction (P_1) and unreactive scattering (P_0) can be written as

$$P_1(\epsilon) = \left(\frac{v_F}{v_{F_2}}\right)\left(\frac{\sigma_{F_2\rightarrow F^+}}{\sigma_{F\rightarrow F^+}}\right)\left(\frac{S_{19}(\epsilon)}{S_{19}(\infty)} - \frac{S_{38}(\epsilon)}{S_{38}(\infty)}\right), \tag{2.1}$$

$$P_0(\epsilon) = \frac{S_{38}(\epsilon)}{S_{38}(\infty)}, \tag{2.2}$$

where ϵ is the exposure in ML F atom, v is the average velocity, σ is the ionization cross section, and S is the mass spectrometer signal of the scattered particle denoted by the subscript. The probability of two atom adsorption is determined by normalization of the three channels

$$P_2(\epsilon) = 1 - P_0(\epsilon) - P_1(\epsilon). \tag{2.3}$$

Having obtained $P_1(\epsilon)$ and $P_2(\epsilon)$ as a function of exposure, the fluorine coverage as a function of exposure can be calculated. By definition of the probabilities, there will be $P_1 + 2P_2$ fluorine atoms adsorbed on the surface for each incoming F_2 molecule. Summing over all incoming F_2 molecules, the coverage, $\theta(\epsilon)$, can be written as

$$\theta(\epsilon) = \int_0^{\epsilon} I_{F_2}(0.5P_1(\epsilon) + P_2(\epsilon))\,d\epsilon, \tag{2.4}$$

where I_{F_2} is the incident F_2 flux in ML F atom/s.

The results shown in Fig. 1 represent the average of the six sets of data shown in Fig. 13 of Ref. 1. Because the incident F_2 flux, and therefore, the F_2 exposure over a fixed integration time in Eq. (2.4), varied from data set to data set, the reaction probabilities and coverage determined from each of the six data sets are interpolated over a common exposure range (0–15 ML F) and interval (0.1 ML F) using a linear interpolation algorithm prior to averaging the six data sets.[7] The error bars shown in Fig. 1 represent the typical uncertainty of a single set of data. The large uncertainty in P_1 and P_2 and consequently the fluorine coverage is due to the large uncertainty in the value[8] for the F atom ionization cross section, $\sigma_{F\rightarrow F^+}$.

III. DESCRIPTION OF MODEL

A. Probability equations

The statistical model, specifically referred to as the four-site model in Sec. IV A 5 a, treats the interaction of the incident F_2 molecule and its complementary F atom with four types of possible sites on the Si(100)(2×1) surface: Sites that are members of filled dimers and hence necessarily occupied, the occupied and unoccupied sites of half-filled dimers, and sites that are member of empty dimers and hence necessarily unoccupied. Thus, a site is distinguished not only by its fluorine occupation, but also by the occupation of its complementary surface dimer atom. The number of sites that are members of a filled dimer is denoted by θ_2, whose value ranges from zero on the clean surface to a maximum of 1 ML at the saturation coverage when every site and consequently when every dimer is filled. The number of occupied sites that are members of a half-filled dimer is denoted by θ_1, as is the number of unoccupied sites that are members of a half-filled dimer. The value of θ_1 ranges from zero on the clean surface to a maximum of 0.5 ML when every dimer is half-filled. Finally, sites that are members of an empty dimer are unoccupied sites. Their number is denoted by $1-(2\theta_1+\theta_2)$. The factor of two in the $2\theta_1$ term arises because both the occupied sites on half-filled dimers and the unoccupied sites on half-filled dimers decrease by θ_1 the number of unoccupied sites that are members of empty dimers. The total coverage, θ, is the sum of the number of occupied sites that are members of both the half-filled and filled dimers, $\theta_1+\theta_2$.

The model treats the interaction of a F_2 molecule incident on a Si(100) surface as a sequential combination of up to three steps, each with two possible outcomes:

1. *Interaction of the F_2 molecule with the surface* leading to either abstraction of the first F atom from the F_2 molecule or unreactive scattering.

2. Assuming F atom abstraction, *the trajectory of the complementary F atom* leads to either direct scattering into the gas phase or the subsequent interaction of the complementary F atom with the surface.

3. Assuming the complementary F atom is not directly scattered into the gas phase, *the interaction of the F atom with the surface* leads to either adsorption or scattering of the complementary F atom.

A pictorial representation of Step 1, the initial interaction of F_2 with the four types of sites, and its two possible outcomes, F atom abstraction or F_2 unreactive scattering, is shown in the first column of Fig. 2. Cross sections *A, B, B*, C, K, M, M*, N* are defined for the two possible outcomes of

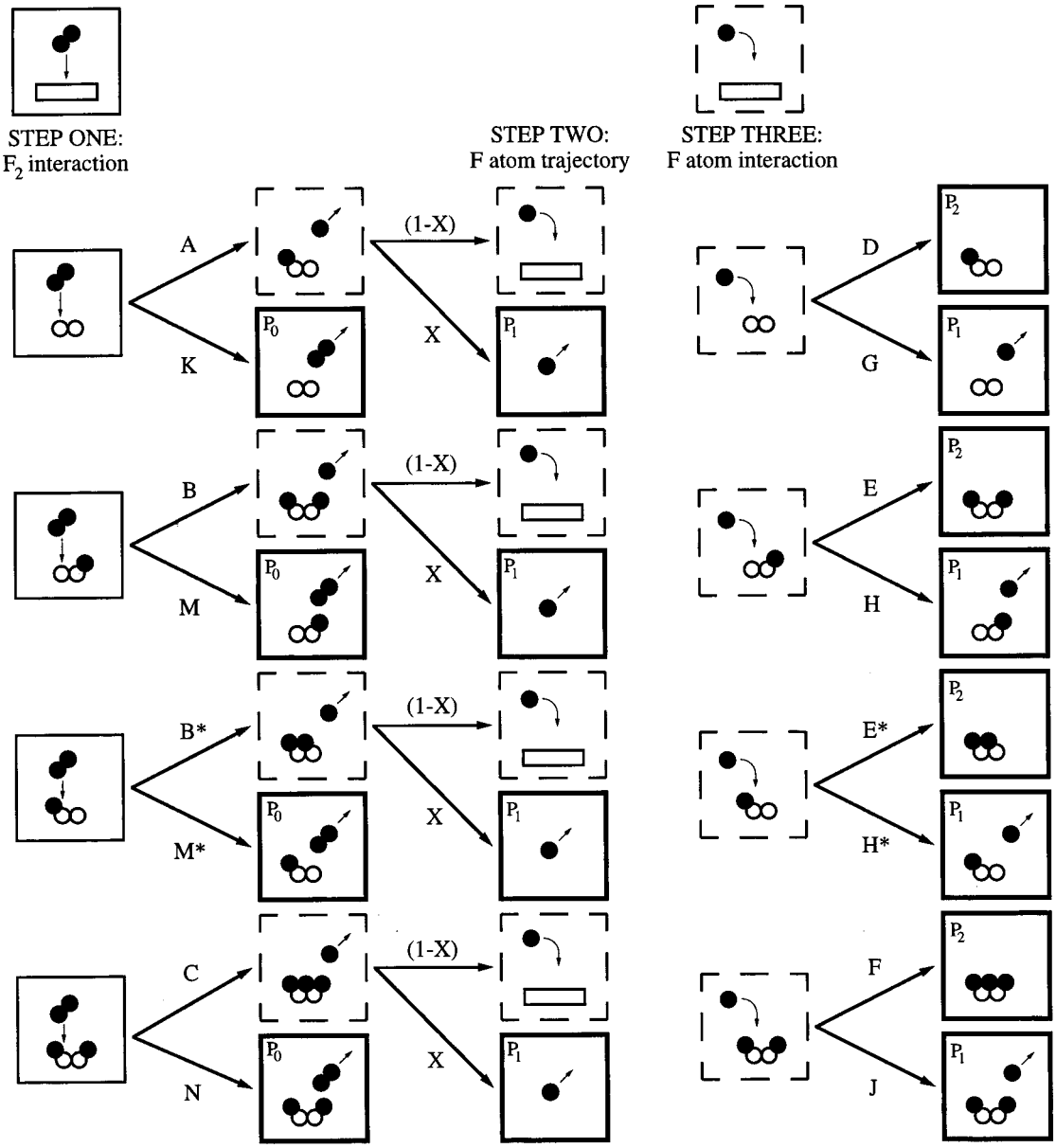

FIG. 2. Pictorial representation of all pathways for interaction of F_2 with Si(100)(2×1) based on model described in text. Solid circles represent F atoms and pairs of hollow circles represent Si dimers. Dashed squares represent intermediate states and thick solid squares represent final states in a pathway.

the initial interaction that can occur on any type of site.

$A \equiv$Cross section for F abstraction from incident F_2 by a site in an empty dimer;

$B \equiv$Cross section for F abstraction from incident F_2 by unoccupied site in half-filled dimer;

$B^* \equiv$Cross section for F abstraction from incident F_2 by occupied site in half-filled dimer;

$C \equiv$Cross section for F atom abstraction from incident F_2 by a site in filled dimer;

$K \equiv$Cross section for unreactive scattering of an incident F_2 by a site in an empty dimer;

$M \equiv$Cross section for unreactive scattering of incident F_2 by unoccupied site in half-filled dimer;

$M^* \equiv$Cross section for unreactive scattering of incident F_2 by occupied site in half-filled dimer;

$N \equiv$Cross section for unreactive scattering of an incident F_2 by a site in a filled dimer.

Relationships between the cross sections A and K, cross sections B, B^*, M, and M^*, and cross sections C and N exist and are derived below. The probability of an outcome is the product of the cross section and the number of sites that are one of the four possible types.

Upon abstraction, the trajectory of the complementary F atom, labeled as Step 2 in Fig. 2, may lead it either to scatter directly into the gas phase, called direct scattering, or to interact with the surface. A probability X is defined as the fraction of the complementary F atoms that directly scatter into the gas phase leading to single atom abstraction (P_1).

The fraction $(1-X)$ of the complementary F atoms that do not directly scatter into the gas phase interact with the surface, labeled as Step 3 in Fig. 2. This interaction may lead to adsorption of the F atom, resulting in two atom adsorption (P_2). If adsorption does not occur, then the F atom is scat-

tered into the gas phase, resulting in single atom abstraction (P_1). Cross sections D, E, E^*, F, G, H, H^*, J are defined for the two possible outcomes of this step that can occur on any of the four types of sites.

D≡Cross section for subsequent F atom adsorption by a site in an empty dimer;

E≡Cross section for subsequent F atom adsorption by unoccupied site in half-filled dimer;

E^*≡Cross section for subsequent F atom adsorption by occupied site in half-filled dimer;

F≡Cross section for F atom adsorption by a site in filled dimer;

G≡Cross section for scattering F atom by a site in an empty dimer;

H≡Cross section for scattering F atom by unoccupied site in half-filled dimer;

H^*≡Cross section for scattering F atom by occupied site in half-filled dimer;

J≡Cross section for scattering F atom by a site in a filled dimer.

Again, relationships between the cross sections D and G, cross sections E, E^*, H, and H^*, and cross sections F and J exist and are derived below.

The probability of a specific pathway in the interaction of F_2 with Si(100) is described by the product of the probabilities for the unique sequence of outcomes for the three individual steps, interaction of F_2 with Si, the trajectory of the complementary F atom, and the interaction of the complementary F atom with Si, on the four distinct sites. The probability of a specific process—two atom adsorption (P_2), single atom abstraction (P_1), and unreactive scattering (P_0)—is the sum of the probabilities for all of the pathways resulting in the adsorption of two F atoms, one F atom, and no F atoms, respectively.

Given these considerations, the probability of unreactive scattering (P_0) is the sum of the individual probabilities for the four pathways leading to unreactive scattering

$$P_0 = K(1-(2\theta_1+\theta_2)) + M\theta_1 + M^*\theta_1 + N\theta_2. \tag{3.1}$$

The terms, in the order in which they are shown, represent the probability for F_2 to unreactively scatter from a site that is a member of an empty dimer, to unreactively scatter from an unoccupied site of a half-filled dimer, to unreactively scatter from an occupied site of a half-filled dimer and to unreactively scatter from a site that is a member of a filled dimer, respectively. Because no complementary F atom is produced during unreactive scattering, there is no need to consider the subsequent complementary F atom dynamics.

The probability of two atom adsorption (P_2) is the sum of the individual probabilities for the sixteen pathways leading to two atom adsorption

$$\begin{aligned}
P_2 = {} & A(1-(2\theta_1+\theta_2))(1-X)D(1-(2\theta_1+\theta_2)) + A(1-(2\theta_1+\theta_2))(1-X)E\theta_1 \\
& + A(1-(2\theta_1+\theta_2))(1-X)E^*\theta_1 + A(1-(2\theta_1+\theta_2))(1-X)F\theta_2 + B\theta_1(1-X) \\
& \times D(1-(2\theta_1+\theta_2)) + B\theta_1(1-X)E\theta_1 + B\theta_1(1-X)E^*\theta_1 + B\theta_1(1-X)F\theta_2 \\
& + B^*\theta_1(1-X)D(1-(2\theta_1+\theta_2)) + B^*\theta_1(1-X)E\theta_1 + B^*\theta_1(1-X)E^*\theta_1 + B^*\theta_1(1-X)F\theta_2 \\
& + C\theta_2(1-X)D(1-(2\theta_1+\theta_2)) + C\theta_2(1-X)E\theta_1 + C\theta_2(1-X)E^*\theta_1 + C\theta_2(1-X)F\theta_2.
\end{aligned} \tag{3.2}$$

The sixteen pathways are all of the possible combinations for the two essential outcomes, F atom abstraction and F atom adsorption, occurring at each of the four possible sites: A filled dimer site, an occupied or unoccupied site of a half-filled dimer and an empty dimer site. For example, the first term in P_2, which constitutes the probability of the pathway involving atom abstraction on a site of an empty dimer followed by a trajectory of the complementary F atom interacting with the surface and subsequent adsorption on a site of an empty dimer, is given by the probability for abstraction on a site of an empty dimer $[A(1-(2\theta_1+\theta_2)]$, multiplied by the probability of an interacting trajectory $(1-X)$ and multiplied by the probability of adsorption of the complementary F atom on a site of an empty dimer $[D(1-(2\theta_1+\theta_2)]$. Since two atom adsorption requires F atom abstraction from the F_2 molecule and the subsequent adsorption of the complementary F atom, none of the pathways resulting in two atom adsorption include direct scattering of the complementary F atom with its probability X, an outcome that necessarily prevents adsorption of the complementary F atom.

Single atom abstraction requires F atom abstraction from the F_2 molecule, but the complementary F atom cannot adsorb to the surface. Sixteen of the pathways resulting in single atom abstraction are similar to the sixteen pathways resulting in two atom adsorption described in Eq. (3.2), except that the complementary F atom scatters from the surface instead of adsorbing onto it. However, unlike two atom adsorption, there are four additional pathways that include direct scattering of the complementary F atom, an outcome that necessarily results in single atom abstraction. The probability of single atom abstraction (P_1) is the sum of the individual probabilities for the twenty pathways leading to single atom abstraction:

$$P_1 = A(1-(2\theta_1+\theta_2))(1-X)G(1-(2\theta_1+\theta_2)) + A(1-(2\theta_1+\theta_2))(1-X)H\theta_1 + A(1-(2\theta_1+\theta_2))(1-X)H^*\theta_1 + A(1-(2\theta_1+\theta_2))(1-X)J\theta_2 + B\theta_1(1-X) \times G(1-(2\theta_1+\theta_2)) + B\theta_1(1-X)H\theta_1 + B\theta_1(1-X)H^*\theta_1 + B\theta_1(1-X)J\theta_2 + B^*\theta_1(1-X) \times G(1-(2\theta_1+\theta_2)) + B^*\theta_1(1-X)H\theta_1 + B^*\theta_1(1-X)H^*\theta_1 + B^*\theta_1(1-X)J\theta_2 + C\theta_2(1-X)G(1-(2\theta_1+\theta_2)) + C\theta_2(1-X)H\theta_1 + C\theta_2(1-X)H^*\theta_1 + C\theta_2(1-X)J\theta_2 + A(1-(2\theta_1+\theta_2))X + B\theta_1X + B^*\theta_1X + C\theta_2X. \quad (3.3)$$

The first sixteen terms represent pathways for the two outcomes, F atom abstraction and the interaction of the complementary F atom with the surface, occurring at each of the four distinguishable sites. The last four terms represent pathways for F atom abstraction on any of the four distinguishable sites followed by direct scattering of the complementary F atom.

This statistical representation of the reaction probabilities given in Eqs. (3.1)–(3.3) assumes that both the F_2 molecule and the F atom, if produced by the initial atom abstraction, only interact one time with the surface. Physically, this assumption rules out the presence of a mobile precursor, either intrinsic or extrinsic. In addition, this representation assumes that the cross sections are independent of coverage. The validity of these assumptions is discussed in Sec. IV C.

The reaction probabilities given in Eqs. (3.1)–(3.3) are simplified by grouping the components of each of the three individual steps that comprise an overall pathway for the interaction of F_2 with Si(100)

$$P_2 = [A(1-(2\theta_1+\theta_2)) + (B+B^*)\theta_1 + C\theta_2](1-X) \times [D(1-(2\theta_1+\theta_2)) + (E+E^*)\theta_1 + F\theta_2], \quad (3.4)$$

$$P_1 = [A(1-(2\theta_1+\theta_2)) + (B+B^*)\theta_1 + C\theta_2](1-X) \times \left[G(1-(2\theta_1+\theta_2)) + (H+H^*)\theta_1 + J\theta_2 + \left(\frac{X}{1-X}\right)\right], \quad (3.5)$$

$$P_0 = K(1-(2\theta_1+\theta_2)) + (M+M^*)\theta_1 + N\theta_2. \quad (3.6)$$

The reaction probabilities given in Eqs. (3.4)–(3.6) are further simplified by incorporating the experimental observation that the initial F atom abstraction cannot occur if the incident F_2 interacts with a filled site. Specifically, the experimental results[1] show that the 1 ML of dangling bonds on the Si(100) surface are the only sites for abstraction and adsorption and that a F_2 molecule must unreactively scatter from a saturated surface so that $P_2(\theta=1\text{ ML})=0$, $P_1(\theta=1\text{ ML})=0$, and $P_0(\theta=1\text{ ML})=1$. Therefore, it is necessary that $B^*=0$ and $C=0$ in Eqs. (3.4)–(3.6). Analogously, if the complementary F atom interacts with a filled site, then F atom adsorption cannot occur. To satisfy this assumption, it is necessary that $E^*=0$ and $F=0$ in Eqs. (3.4)–(3.6) leading to

$$P_2 = [A(1-(2\theta_1+\theta_2)) + B\theta_1](1-X) \times [D(1-(2\theta_1+\theta_2)) + E\theta_1], \quad (3.7)$$

$$P_1 = [A(1-(2\theta_1+\theta_2)) + B\theta_1](1-X) \times \left[G(1-(2\theta_1+\theta_2)) + (H+H^*)\theta_1 + J\theta_2 + \left(\frac{X}{1-X}\right)\right], \quad (3.8)$$

$$P_0 = K(1-(2\theta_1+\theta_2)) + (M+M^*)\theta_1 + N\theta_2. \quad (3.9)$$

If there are only three possible channels through which a F_2 molecule incident on a Si(100) surface may interact, then the sum of their probabilities described by Eqs. (3.7)–(3.9) must be unity

$$P_{\text{total}} = P_0 + P_2 + P_1 = 1. \quad (3.10)$$

In addition, the sum of the probabilities for every outcome in a given step must be unity. Specifically, in Step 1 shown in Fig. 2, the sum of the probabilities of the eight outcomes, either F atom abstraction or F_2 unreactive scattering, must be unity:

$$P_{\text{Step 1}} = A(1-(2\theta_1+\theta_2)) + B\theta_1 + K(1-(2\theta_1+\theta_2)) + (M+M^*)\theta_1 + N\theta_2 = 1. \quad (3.11)$$

Alternatively, Eq. (3.11) can be rationalized in the following manner: The first step in the interaction of F_2 with Si(100) is the F atom abstraction from F_2 or the unreactive scattering of F_2. The probability of F atom abstraction from the incident F_2 molecule is given by

$$P_{\text{abstraction}} = [A(1-(2\theta_1+\theta_2)) + B\theta_1]. \quad (3.12)$$

If the initial abstraction does occur, the resulting overall event must be either two atom adsorption (P_2) or single atom abstraction (P_1) but it cannot result in unreactive scattering (P_0). So, if the initial abstraction does not occur, the incident F_2 must unreactively scatter. Therefore, the absence of the initial abstraction is the sole contribution to unreactive scattering (P_0) so that

$$P_0 = [K(1-(2\theta_1+\theta_2)) + (M+M^*)\theta_1 + N\theta_2] = 1 - [A(1-(2\theta_1+\theta_2)) + B\theta_1], \quad (3.13)$$

which is equivalent to Eq. (3.11) After some algebra, Eq. (3.13) becomes

$$(K+A-1) + (M+M^*+B-2A-2K)\theta_1 + (N-K-A)\theta_2 = 0, \quad (3.14)$$

resulting in a system of three equations

$$K+A-1=0,$$

$$M+M^*+B-2A-2K=0, \quad N-K-A=0. \tag{3.15}$$

These equalities constrain the cross sections A relative to K, as well as B relative to $M+M^*$

$$K=1-A, \tag{3.16}$$

$$M+M^*=2-B. \tag{3.17}$$

The equality also yields the value of the cross section N

$$N=1. \tag{3.18}$$

Because of these constraints, the cross section K and the sum of cross sections $M+M^*$ are justifiably eliminated from the model.

In an analogous manner, the sum of the probabilities for the eight distinct outcomes for either F atom adsorption or F atom direct scattering of Step 3 in Fig. 2 must be unity

$$P_{\text{Step 3}}=D(1-(2\theta_1+\theta_2))+E\theta_1+G(1-(2\theta_1+\theta_2)) +(H+H^*)\theta_1+J\theta_2=1. \tag{3.19}$$

After some algebra, Eq. (3.19) becomes

$$(D+G-1)+(E+H+H^*-2D-2G)\theta_1 +(J-D-G)\theta_2=0, \tag{3.20}$$

resulting in a system of three equations:

$$D+G-1=0,$$

$$E+H+H^*-2D-2G=0, \quad J-D-G=0. \tag{3.21}$$

These equalities constrain the cross sections G relative to D, as well as $H+H^*$ relative to E

$$G=1-D, \tag{3.22}$$

$$H+H^*=2-E. \tag{3.23}$$

The equality also yields the value of the cross section J,

$$J=1. \tag{3.24}$$

Because the normalization relationships lead to redundant cross sections, the cross sections G and $H+H^*$ are justifiably eliminated from the model. Substituting Eqs. (3.22)–(3.24) into Eqs. (3.7) and (3.8) yields

$$P_2=[A(1-(2\theta_1+\theta_2))+B\theta_1](1-X) \times[D(1-(2\theta_1+\theta_2))+E\theta_1], \tag{3.25}$$

$$P_1=[A(1-(2\theta_1+\theta_2))+B\theta_1](1-X) \times\left[1-[D(1-(2\theta_1+\theta_2))+E\theta_1]+\left(\frac{X}{1-X}\right)\right]. \tag{3.26}$$

Redistributing the $(1-X)$ factor and incorporating it into the cross sections D and E allows the probability factor X to be eliminated from the probability equations

$$P_2=[A(1-(2\theta_1+\theta_2))+B\theta_1] \times[D'(1-(2\theta_1+\theta_2))+E'\theta_1], \tag{3.27}$$

$$P_1=[A(1-(2\theta_1+\theta_2))+B\theta_1] \times[1-[D'(1-(2\theta_1+\theta_2))+E'\theta_1]], \tag{3.28}$$

$$P_0=1-[A(1-(2\theta_1+\theta_2))+B\theta_1], \tag{3.29}$$

where the new cross sections D' and E' are related to the original cross sections D and E by:

$$D'\equiv D(1-X), \tag{3.30}$$

$$E'\equiv E(1-X). \tag{3.31}$$

The resulting simplified probability equations, Eqs. (3.27)–(3.29) have an appealingly straightforward interpretation. The first factor in P_2 is given by Eq. (3.12) and is the probability of F atom abstraction from an incident F_2 molecule. This factor is multiplied by the probability of adsorption of the complementary F atom to yield the total probability for two atom adsorption, P_2. Likewise, P_1 is the product of the probability of F atom abstraction and the probability of the complementary F atom *not* adsorbing, or one minus the probability of it adsorbing. The probability of unreactive scattering, P_0, is one minus the probability of F atom abstraction, as noted in the discussion of Eq. (3.13).

B. Coverage equations

The solution of Eqs. (3.27)–(3.29) for the three probabilities depends on knowledge of the number of the occupied sites in half-filled dimers, θ_1, and the number of occupied sites in filled dimers, θ_2, as a function of F_2 exposure. However, these two types of occupied sites are not distinguishable in these experiments described above. Instead, the simplifying assumption is made that the occupancy of each type of site develops randomly. Starting from a clean surface, the initial infinitesimal fluorine coverage arises from the number of F atoms adsorbed via a statistical distribution of pathways at zero coverage over an infinitesimal exposure range. Once a F atom is adsorbed on a site, it does not diffuse or desorb. The coverage increases by iteratively considering the distribution of pathways at the new coverage. Mathematically, the coverage is the integral over exposure of the product of the incident F_2 flux and the probability for each relevant reaction pathway weighted by the number of F atoms adsorbed along each pathway. Thus, the number of occupied sites in a half-filled dimer, θ_1, is the sum of contributions from the pathways leading to two atom adsorption (P_2) and single atom abstraction (P_1) that create half-filled dimers minus the contributions from the pathways that destroy half-filled dimers by creating filled dimers

$$\theta_1(\epsilon)=\frac{1}{2}I_{F_2}\int \{2A(1-(2\theta_1+\theta_2))D'(1-(2\theta_1+\theta_2)) +A(1-(2\theta_1+\theta_2))[1-[D'(1-(2\theta_1+\theta_2)) +E'\theta_1]]-2B\theta_1E'\theta_1-B\theta_1[1-[D'(1-(2\theta_1 +\theta_2))+E'\theta_1]]\}d\epsilon, \tag{3.32}$$

which simplifies to

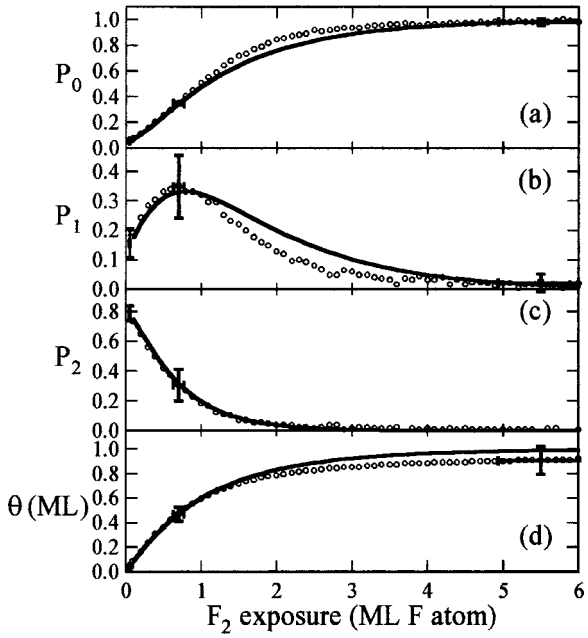

FIG. 3. Reaction probability of F_2 with Si(100) as a function of F_2 exposure for (a) unreactive scattering P_0, (b) single atom abstraction P_1, and (c) two atom adsorption P_2 derived from best fit of model to data. (d) Fluorine coverage as a function of F_2 exposure. Data (hollow circles), taken from Fig. 1, are plotted as a function of F_2 exposure instead of fluorine coverage. Error bars on exposure reflect uncertainty in beam flux.

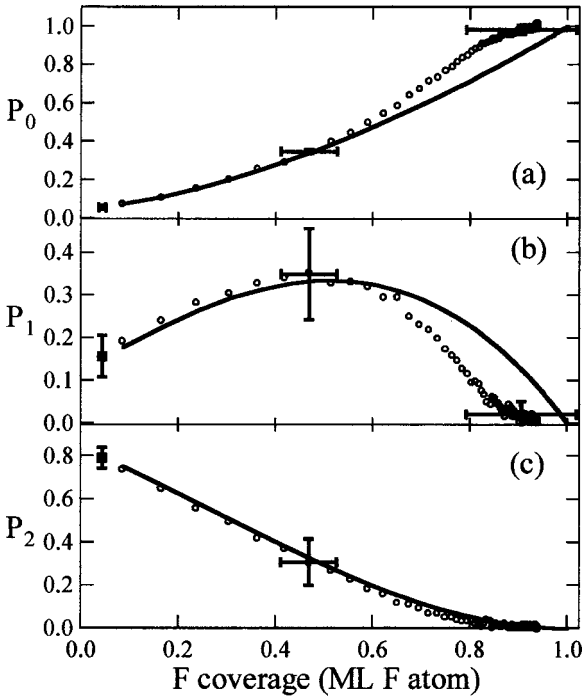

FIG. 4. Reaction probability of F_2 with Si(100) as a function of fluorine coverage for (a) unreactive scattering P_0, (b) single atom abstraction P_1, and (c) two atom adsorption P_2 derived from best fit of model to data. Data (hollow circles) from Fig. 1.

$$\theta_1(\epsilon)=\frac{1}{2}I_{F_2}\int \{A(1-(2\theta_1+\theta_2)) \times[1+D'(1-(2\theta_1+\theta_2))-E'\theta_1]-B\theta_1 \times[1-D'(1-(2\theta_1+\theta_2))+E'\theta_1]\}d\epsilon. \tag{3.33}$$

The number of occupied sites that are members of a filled dimer, θ_2, is the sum of the contributions from two atom adsorption and single atom abstraction (P_1) to create filled dimers

$$\theta_2(\epsilon)=I_{F_2}\int \{A(1-(2\theta_1+\theta_2))E'\theta_1+B\theta_1D' \times(1-(2\theta_1+\theta_2))+2B\theta_1E'\theta_1+B\theta_1 \times[1-[D'(1-(2\theta_1+\theta_2))+E'\theta_1]]\}d\epsilon, \tag{3.34}$$

which simplifies to

$$\theta_2(\epsilon)=I_{F_2}\int \{A(1-(2\theta_1+\theta_2))E'\theta_1+B\theta_1(1+E'\theta_1)\}d\epsilon. \tag{3.35}$$

The total coverage, an experimentally determined quantity, is the sum of $\theta_1+\theta_2$

$$\theta(\epsilon)=I_{F_2}\int \{\tfrac{1}{2}\{A(1-(2\theta_1+\theta_2))[1+D'(1-(2\theta_1+\theta_2)) -E'\theta_1]\}\}-\tfrac{1}{2}\{B\theta_1[1-D'(1-(2\theta_1+\theta_2))+E'\theta_1]\} +\{A(1-(2\theta_1+\theta_2))E'\theta_1+B\theta_1(1+E'\theta_1)\}d\epsilon, \tag{3.36}$$

which simplifies to

$$\theta(\epsilon)=\frac{1}{2}I_{F_2}\int [A(1-(2\theta_1+\theta_2))+B\theta_1] \times[1+D'(1-(2\theta_1+\theta_2))+E'\theta_1]d\epsilon. \tag{3.37}$$

The coverage equations for θ_1 and θ_2 [Eqs. (3.33) and (3.35)] are verified by checking that Eq. (3.37) is equal to the integral of the product of the sum of the weighted probabilities and the incident flux

$$\theta(\epsilon)=I_{F_2}\int (P_2+\tfrac{1}{2}P_1)d\epsilon. \tag{3.38}$$

The validity of the constraints on diffusion and desorption as well as on the homogeneity of the spatial distribution of adsorbed F atoms that are inherent in the development of the coverage equations is discussed in Sec. IV B.

C. Fitting algorithm and measure of the goodness of fit

There are four unique cross sections, A, B, D', and E' in the three equations for the reaction probabilities. The values of two of the factors can be determined from the experimental data in the limit of zero coverage

$$P_2(\theta=0)=AD'=0.83\pm0.03, \tag{3.39}$$

$$P_1(\theta=0)=A(1-D')=0.13\pm0.03, \tag{3.40}$$

$$P_0(\theta=0)=1-A=0.04\pm0.03. \tag{3.41}$$

Therefore,

$$A=0.96\pm0.03 \tag{3.42}$$

and

$$D' = 0.87 \pm 0.04. \tag{3.43}$$

Thus, there are two parameters, cross sections B and E', that are adjusted to fit the model to the experimental measurements of the probabilities. The probabilities are calculated by numerically solving the system of coupled differential equations for θ_1 and θ_2, described by Eqs. (3.33) and (3.35), respectively, and substituting these solutions into the equations for the reaction probabilities, Eqs. (3.27)–(3.29). Figure 3 is a plot of the three reaction probabilities and the coverage [Eq. (3.37)] as a function of F_2 exposure, derived from the best fit of the model to the data. The best fit values are $B = 1.68 \pm 0.06$ and $E' = 1.03 \pm 0.14$, where the uncertainties represent the standard deviation of the fitting parameters.[7] Figure 4 shows the same reaction probabilities as in Figs. 3(a)–3(c) but plotted as a function of fluorine coverage. The model is fit to the interpolated and averaged experimental data described in Sec. II using the Levenberg–Marquardt least-squares nonlinear fitting algorithm.

The goodness of fit is determined by a chi square (χ^2) function that is defined as the sum of the individual χ^2 values of the two independent functions, the probability of unreactive scattering (P_0) and the probability of single atom abstraction (P_1)

$$\chi^2 = \sum_{i=1}^{10} \left[\left(\frac{P_0^{\text{obs}}(\epsilon_i) - P_0^{\text{exp}}(\epsilon_i)}{\sigma_{P_0}(\epsilon_i)} \right)^2 + \left(\frac{P_1^{\text{obs}}(\epsilon_i) - P_1^{\text{exp}}(\epsilon_i)}{\sigma_{P_1}(\epsilon_i)} \right)^2 \right]. \tag{3.44}$$

The uncertainties in $P_0(\epsilon_i)$ and $P_1(\epsilon_i)$, denoted as $\sigma_{P_0}(\epsilon_i)$ and $\sigma_{P_1}(\epsilon_i)$, respectively, are representative of the uncertainties for a single set of data as described in Sec. II. The χ^2 function is evaluated over the first 1 ML F exposure. A χ^2 value of 3.4 is obtained for $B = 1.68$ and $E' = 1.03$. A search over the two-dimensional phase space performed by randomly selecting starting values for B and E' ranging from 0%–200% of the best fit values consistently converged at the best fit values confirming that the fit corresponded to a global minimum in the χ^2 function. Over the exposure range defined by the summation in χ^2 of Eq. (3.44), there are twenty degrees of freedom corresponding to the ten values each for $P_0(\epsilon_i)$ and $P_1(\epsilon_i)$. The minimum χ^2 value is significantly less than the number of degrees of freedom, satisfying the standard criterion for the appropriateness of using a certain model to describe a given set of data.[9] However, the data and the fit to the data do not match well at exposures above 1 ML, which is outside of the range over which the χ^2 value is calculated. The discrepancy between the model and the data at high exposures and consequently at high coverages is discussed below.

IV. DISCUSSION

The model provides a reasonably accurate description of the kinetics of the interaction of low energy F_2 with Si(100) at 250 K. The model treats the two dissociative chemisorption channels, single atom abstraction and two atom adsorption, as a series of three distinct steps. The initial step, the abstraction and adsorption of the first F atom from the incident F_2 molecule, is common to both channels while the outcomes of the second and third steps, the trajectory of the complementary F atom and its interaction with the surface, distinguishes between the two channels. The fate of the complementary F atom is independent of the abstraction and adsorption of the first F atom because the energy liberated by one Si–F bond is sufficient to overcome the bond energy in the incident F_2 molecule. Second, the reactivity of a dangling bond site is dependent not only on its occupancy, but on the occupancy of the complementary atom in the dimer on the Si(100)(2×1) surface. The purpose of the discussion is to provide further evidence and justification for the physical reasonableness and plausibility of the model and to gain insight into the dynamics of the interaction of F_2 with Si(100).

A. Physical implications of the model

1. Total cross sections for reaction

A cross section is a common concept in gas-phase scattering dynamics and represents the ''target area'' that one particle presents to another particle in a specific scattering event. It is a valuable quantity because it describes the likelihood of a reaction in terms of collision trajectories. Given equal opacity functions, a small cross section implies a head-on, small impact parameter collision for the scattering event to occur, whereas a large cross section implies attractive forces that bring the colliding particles together even if the two particles do not appear to be on a collision course.

The cross section is related to the rate of a reaction by the concentration and velocity of the reactants. For the prototypical gas-phase reaction $A + B \rightarrow C$, the rate of production of C is given by

$$\frac{dn_c}{dt} = \int_{v_A} \int_{v_B} v \sigma(v) n_A f(v_A) n_B f(v_B) dv_A dv_B, \tag{4.1}$$

where v is the relative velocity ($v_A - v_B$) between A and B, $\sigma(v)$ is the cross section for reaction, and n_x, v_x, and $f(v_x)$ are the number density, velocity, and velocity distribution of particle X, respectively. In the case of F_2 interacting with Si, the Si is stationary so the relative velocity v is equivalent to the velocity of F_2, v_{F_2}, which is approximately monoenergetic in a supersonic beam so the integration over velocity can be ignored. Therefore, by analogy to a gas-phase scattering event, the rate of unreactive scattering from a site on a filled dimer is:

$$\text{rate of unreactive scattering} = v_{F_2} \sigma_N n_{F_2} n_{Si}^{\text{filled dimer}}, \tag{4.2}$$

where $n_{Si}^{\text{filled dimer}}$ is the two-dimensional number density of occupied sites in a filled dimer. Note that the product of the velocity and the F_2 number density is simply the flux of F_2

$$\text{rate of unreactive scattering} = I_{F_2} \sigma_N n_{Si}^{\text{filled dimer}}. \tag{4.3}$$

The cross sections A, B, D', and E' determined from the fit of this model to the data and the cross sections K, $M + M^*$, N, G, $H + H^*$, and J, determined from relationships to the independent cross sections, are related to their gas-phase counterparts, σ_A, σ_B, $\sigma_{D'}$, $\sigma_{E'}$, σ_K, $\sigma_M + \sigma_{M^*}$, σ_N, σ_G, $\sigma_H + \sigma_{H^*}$, and σ_J, respectively. For example, the

probability of unreactive scattering of F_2 from a site of a filled dimer is the product of the cross section N and the fraction of the total sites that are members of filled dimers:

$$P_{\text{unreactive}}^{\text{filled dimer}} = N\left(\frac{n_{\text{Si}}^{\text{filled dimer}}}{n_{\text{Si}}^{\text{total}}}\right). \tag{4.4}$$

The cross section N is related to the rate of unreactive scattering from a filled dimer site because the rate is the product of the probability of unreactive scattering and the flux of incident F_2 molecules:

$$\text{rate of unreactive scattering} = I_{F_2} P_{\text{unreactive}}^{\text{filled dimer}} = I_{F_2} N\left(\frac{n_{\text{Si}}^{\text{filled dimer}}}{n_{\text{Si}}^{\text{total}}}\right). \tag{4.5}$$

A comparison of Eq. (4.5) with Eq. (4.3) yields a relationship between the cross section N and its gas-phase counterpart, σ_N

$$\sigma_N = \frac{N}{n_{\text{Si}}^{\text{total}}}. \tag{4.6}$$

Equivalent relationships hold for all the cross sections in the model. The quantity, $n_{\text{Si}}^{\text{total}}$, is the two-dimensional density of dangling bond sites, either occupied or unoccupied, on the Si(100) surface. Based on a unit cell lattice spacing of 3.84 Å, it has a value of $n_{\text{Si}}^{\text{total}} = 6.78\times10^{14}\,\text{cm}^{-2}$. The inverse of this quantity, $1/n_{\text{Si}}^{\text{total}} = 14.7\times10^{-16}\,\text{cm}^2$, is the cross-sectional area of a Si(100) surface site.

In the development of the model, the cross section N for unreactive scattering of F_2 from an occupied site of a filled dimer is determined to be equal to one which yields a value of $14.7\times10^{-16}\,\text{cm}^2$ for σ_N. This approximation for σ_N effectively treats the collision radius of F_2 (0.92 Å)[10] as small compared to the radius of a surface site, 2.2 Å, as calculated from its cross-sectional area, $14.7\times10^{-16}\,\text{cm}^2$. Similarly, the cross section J for unreactive scattering of a F atom from an occupied site of a filled dimer is determined to be equal to unity which yields a value of $14.7\times10^{-16}\,\text{cm}^2$ for σ_J. Again, this approximation treats the collision radius of a F atom as small compared to the radius of a surface site. Therefore, the cross sections σ_N and σ_J represent the statistical probability of colliding with the appropriate site.

Similarly, Eq. (4.6) yields values for the cross section for F atom abstraction from a F_2 molecule by an unoccupied site in an empty dimer, $\sigma_A = 14.0\times10^{-16}\,\text{cm}^2$, and by an unoccupied site in a half-filled dimer, $\sigma_B = 24.7\times10^{-16}\,\text{cm}^2$. The cross section for adsorption of the complementary F atom on a site in an empty dimer, $\sigma_{D'}$, is $12.8\times10^{-16}\,\text{cm}^2$ and by a site in a half-filled dimer, $\sigma_{E'}$, is $15.1\times10^{-16}\,\text{cm}^2$. Although these cross sections do not reflect accurate absolute values, their values relative to the cross section of a surface site and their values relative to each other do reveal the relative reactivities of the different sites and different processes in the interaction of F_2 with Si(100).

2. Initial F atom abstraction

The first step in both single atom abstraction and two atom adsorption is the abstraction of a F atom from the incident F_2 molecule. This initial abstraction can only occur on an unoccupied dangling bond site as shown by the experimental results. The good agreement between the model and the data indicates that the reactivity of a given site is dependent on the occupation of its complementary dimer atom. Specifically, the cross section for F atom abstraction from a F_2 molecule by an unoccupied site in a half-filled dimer, σ_B, is $24.7\times10^{-16}\,\text{cm}^2$ and that by a site of an empty dimer, σ_A, is $14.0\times10^{-16}\,\text{cm}^2$. The large values of both cross sections compared to the cross-sectional area of a surface site, $14.7\times10^{-16}\,\text{cm}^2$, suggest that there is no significant energetic barrier to the abstraction of a F atom from a F_2 molecule by a Si dangling bond, in agreement with the experimental observation. In addition, σ_B is larger than the cross-sectional area of a surface site by almost a factor of two. Its larger value implies that the empty site on the half-filled dimer is much more reactive than expected from simple statistical considerations and that the interaction potential between the unoccupied Si dimer atom and the F_2 molecule is attractive. The specific site reactivity is discussed further in Sec. IV A 3.

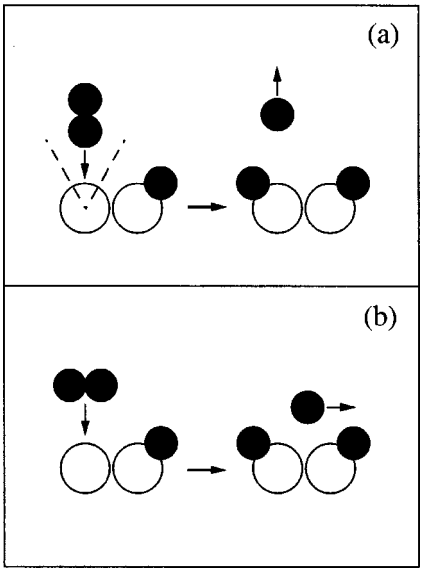

FIG. 5. Pictorial representation of (a) perpendicular and (b) parallel approach geometries of F_2. Dashed line in (a) at 30° with respect to surface normal represents maximum acceptance angle resulting in direct F atom scattering as determined from results of model.

After the initial abstraction occurs, the fate of the complementary F atom, as discussed in the following section, is still unknown. However, regardless of the outcome, dissociative chemisorption has occurred.

3. Neighbor independent single atom abstraction

Single atom abstraction occurs if the complementary F atom does not adsorb to the surface, but remains a gas-phase F atom. Figure 5 shows two limiting scenarios for the trajectory of the F atom that depend on the orientation of the incident F_2 molecule. If the initial abstraction occurs with the F_2 molecular bond axis in a perpendicular approach geometry with respect to the surface plane [Fig. 5(a)], the exothermicity will propel the F atom away from the surface, giving no opportunity for the F atom to interact with it. This mecha-

nism for single atom abstraction is termed ''neighbor independent'' because the complementary F atom scatters into the gas phase regardless of the occupancy of the neighboring sites. This direct scattering into the gas phase is described by the probability X. The value of X cannot be uniquely determined because of its relationship to the other cross sections in the model, but an upper bound can be determined in the following manner. The probability of single atom abstraction in Eq. (3.8) can be written as

$$P_1=[A(1-(2\theta_1+\theta_2))+B\theta_1] \times[G'(1-(2\theta_1+\theta_2))+H'\theta_1+(1-X)\theta_2+X], \tag{4.7}$$

where $J=1$ and the cross sections G' and H' are related to the original factors G and $H+H^*$ by:

$$G'\equiv G(1-X), \quad H'\equiv(H+H^*)(1-X). \tag{4.8}$$

In the limit that the cross section G' for unreactive scattering of a F atom from a site on an empty dimer is vanishingly small, the probability of single atom abstraction at zero coverage simplifies to

$$P_1(\theta=0)=AX=0.13\pm0.03. \tag{4.9}$$

Therefore, if $A=0.96\pm0.03$, then $X=0.13\pm0.03$ is the upper bound for the probability of direct F atom scattering. The above physical picture suggests that the value of X is proportional to the solid angle of molecular orientations leading to direct scattering relative to the 2π steradians of the hemisphere above the surface. From purely geometric considerations, the F_2 molecular axis would have to lie within 30° of the surface normal for single atom abstraction to occur via the direct F atom scattering mechanism.

4. Neighbor-dependent single atom abstraction and two atom adsorption

On the other hand, if the initial abstraction occurs with the molecular axis of the F_2 molecule at angle greater than 30° from the surface normal [Fig. 5(b)], the complementary F atom will scatter along the surface. Because the Si surface is so corrugated, the F atom will probably have only one interaction with the surface. If this interaction occurs at an occupied site, the F atom will be scattered into the gas phase leading to single atom abstraction. However, if this interaction occurs at an unoccupied site, the F atom may either scatter into the gas phase or adsorb on the surface leading to single atom abstraction or two atom adsorption, respectively.

The cross section for F atom adsorption by an unoccupied site on a half-filled dimer, $\sigma_{D'}$, is $15.1\times10^{-16}\,\mathrm{cm}^2$ and that by a site on an empty dimer, $\sigma_{E'}$, is $12.8\times10^{-16}\,\mathrm{cm}^2$. Like the initial F atom abstraction from the incident F_2 molecule, the values of both cross sections are large with respect to the cross-sectional area of a surface site, $14.7\times10^{-16}\,\mathrm{cm}^2$, suggesting that there is no significant energetic barrier to adsorption of a F atom on a Si dangling bond. In fact, the values of $\sigma_{D'}$ and $\sigma_{E'}$ suggest that the F atom will almost always adsorb if it interacts with an empty site leading to two atom adsorption. On the other hand, it is known from the experimental results that the F atom cannot adsorb if it interacts with an occupied site and, therefore, is scattered into the gas phase. This mechanism for single atom abstraction is termed ''neighbor dependent'' because it is dependent on the occupancy of the neighboring sites. It is this mechanism that is responsible for the nonmonotonic parabolic dependence of the probability for single atom abstraction with coverage. In particular, the maximum in P_1 arises from the competition between the number of empty sites necessary to effect the initial F atom abstraction which decreases with coverage and the number of filled sites necessary to prevent the complementary F atom adsorption which increases with coverage. Therefore, given that the probability of neighbor independent single atom abstraction is small, P_1 at low coverage ($\theta<0.5$ ML) is always lower than P_2 because the number of empty sites for F atom adsorption outnumbers the number of filled sites which prevent F atom adsorption. Conversely, at high coverage ($\theta>0.5$ ML), single atom abstraction is the dominant reactive channel. This qualitative observation based on the model is in accordance with the experimental results even at high coverage where the model cannot quantitatively describe the data well. The observation that two atom adsorption is the dominant channel at low coverage is in stark contrast to the conclusions of previous experimental investigations[11] which suggested and theoretical investigations[12] which calculated that single atom abstraction was the dominant channel in the limit of zero coverage.

5. Surface site reactivity

a. Nondifferentiation of sites: two-site model. The importance of the distinguishability of the adsorption sites on the basis of the occupancy of the complementary dimer site for agreement between the model and the data is investigated by carrying out a calculation in which they are not differentiated. Specifically, the effect of not differentiating between the reactivity of empty and half-filled dimers is probed by equating the cross section for F atom abstraction on an unoccupied site of an empty dimer to that of a half-filled dimer, $A=B$, as well as by equating the cross section for adsorption of the complementary F atom on an unoccupied site of an empty dimer to that of a half-filled dimer, $D'=E'$. Incorporating these equalities into Eqs. (3.27)–(3.29) yields simplified equations for P_2, P_1, and P_0, respectively, for what is now effectively a two-site model consisting of occupied and unoccupied sites

$$P_2=AD'(1-\theta)^2, \tag{4.10}$$

$$P_1=A(1-\theta)[1-D'(1-\theta)], \tag{4.11}$$

$$P_0=1-[A(1-\theta)]. \tag{4.12}$$

These probability equations lead to simplified coverage equations [cf. Eqs. (3.33) and (3.35)]

$$\theta_1(\epsilon)=\frac{1}{2}I_{F_2}\int[A(1-\theta)+AD'(1-\theta)^2 -2A\theta_1(1+D'(1-\theta))]d\epsilon, \tag{4.13}$$

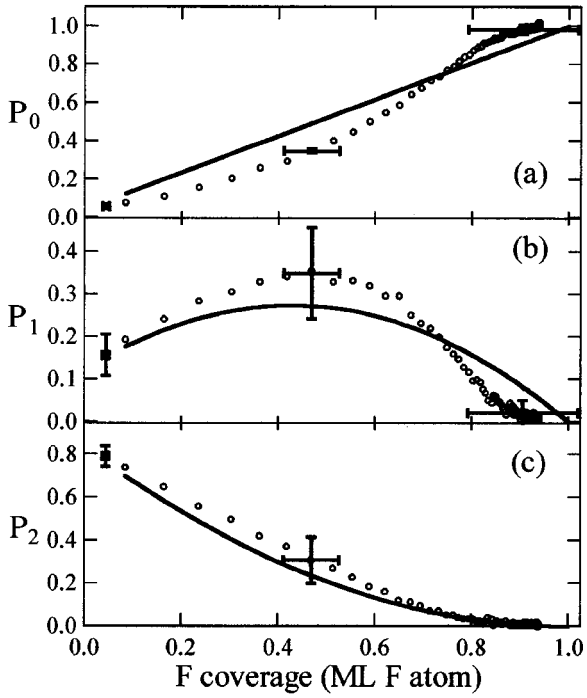

FIG. 6. Reaction probability of F_2 with Si(100) as a function of fluorine coverage for (a) unreactive scattering P_0, (b) single atom abstraction P_1, and (c) two atom adsorption P_2 derived from best fit of model to data without site differentiation, $A=B$, and $D'=E'$. Data (hollow circles) from Fig. 1.

$$\theta_2(\epsilon)=\frac{1}{2}I_{F_2}\int A\theta_1(1+D'(1-\theta))d\epsilon. \tag{4.14}$$

The system of coupled differential equations, Eqs. (4.13) and (4.14), is solved numerically and their solutions are substituted into Eqs. (4.10)–(4.12) to determine the reaction probabilities. There are no adjustable parameters in the two-site model because the two cross sections, A and D', are both determined from the experimentally measured probabilities at zero coverage

$$P_2(\theta=0)=AD'=0.83\pm0.03, \tag{4.15}$$

$$P_1(\theta=0)=A(1-D')=0.13\pm0.03. \tag{4.16}$$

Figures 6(a)–6(c) is a comparison of the reaction probabilities as a function of coverage derived from the two-site model and the experimental results. The two-site model does not describe the data well. The χ^2 value, as defined in Eq. (3.44), is 1012 which is orders of magnitude greater than that from the four-site model. In particular, the two-site model is unable to describe P_0, the probability of unreactive scattering. According to Eq. (4.12), it predicts a linear dependence of P_0 on coverage, in striking contrast to the nonlinear dependence observed experimentally. The contribution of P_0 to the χ^2 function [the first term in Eq. (3.44)] is 1009 for the two-site model compared to 3.1 for the four-site model. Since unreactive scattering is the process that results when F atom abstraction from F_2 does not occur and since F atom abstraction requires one empty site, leading to an expectation of a linear dependence on the number of empty sites, a linear dependence on the number of filled sites or coverage is expected for unreactive scattering. Therefore, the unexpected nonlinearity of the experimental data for P_0 suggests that the reactivity is not described so simply.

However, the two-site model does describe the probability of single atom abstraction, P_1, about as well as the four-site model. The contribution of P_1 to the χ^2 function [the second term in Eq. (3.44)] is 3.1 for the two-site model compared to 0.25 for the four-site model. Both values are much less than 20, the number of degrees of freedom, and therefore are reasonably accurate descriptions of the data over the 0 to 1 ML F exposure range. In contrast, the probability of two atom adsorption, P_2, a value that is dependent on the probability of the other two reaction channels, is inaccurately described by the two-site model. In particular, the two-site model predicts the standard Langmuirian coverage dependence that is quadratic in the number of empty sites, i.e., $(1-\theta)^2$, whereas the data are essentially linear with respect to the number of sites except at high coverages. On the other hand, the four-site model is able to accurately describe P_2. It is a mathematical necessity that the probability of two atom adsorption be essentially quadratic in the number of empty sites because this process requires the adsorption of two atoms on two empty sites. Thus, every term in Eq. (3.2) is the product of two terms that are related to the number of empty sites. However, the differentiation of sites allows the unoccupied sites in empty and half-filled dimers to contribute unequally to two atom adsorption resulting in an overall reaction probability that is quasilinear as opposed to quadratic with respect to the number of empty sites. In contrast, single atom abstraction is dominated by the filled sites preventing the adsorption of the complementary F atom. Unlike single atom abstraction which requires filled sites, which are all equally unreactive, to prevent F atom adsorption, two atom adsorption requires empty sites, which are not equally reactive, for F atom adsorption. Therefore, the two-site model gives a description for single atom abstraction that is similar to that of the four-site model, but it does not for two atom adsorption.

The differentiation between the reactivity of the empty and half-filled dimers yields a dramatic improvement in the goodness of fit of the model to the experimental data, especially with regard to P_0 and P_2. Although the improvement could be a natural consequence of the four-site model having two more adjustable parameters than the two-site model, it will be shown in the next section that there is a physical basis for the differentiation of sites on the Si(100) surface.

b. Dimer pairing energy. The unreconstructed Si(100) surface consists of Si atoms that are sp^3-coordinated to two Si atoms below the surface. The remaining two valence electrons each occupy one of the remaining two sp^3 orbitals of the tetrahedron that project into the vacuum. These singly occupied orbitals are the dangling bonds. The dimerization that occurs in the (2×1) reconstruction of the Si(100) surface is primarily a sigma interaction between one pair of dangling bonds from two surface Si atoms. The remaining two dangling bonds interact weakly through a π interaction.[13] The magnitude of this π interaction is the subject of controversy in the literature.[14–16]

The enhanced reactivity of an unoccupied site in a half-

filled dimer relative to that in an empty dimer for both F atom abstraction and adsorption of the complementary F atom, as evidenced by the larger value of B compared to A and of D' compared to E', can be understood in terms of the stability of the Si dimer. The dimer is destabilized when one of the dangling bonds reacts because there is the loss of the stabilizing π interaction between the two dangling bonds. The unusual first order recombinative desorption kinetics of H_2 from Si(100) has been attributed to the pairing of H atoms on Si dimers to overcome the destabilization of the Si dimer π interaction.[14–16] Models for the kinetics of thermal desorption of H_2 from Si(100) suggest that the driving force behind the pairing of H atoms to completely fill a dimer site is the π-bond stabilization of the unoccupied Si–Si dimers.[14,15] In addition, STM (scanning tunneling microscope) measurements by Boland[16] on the H–Si(100) system show that when H atoms adsorb on the Si(100)(2×1) surface, they tend to occupy both sites on a single dimer rather than a single site on two different dimers. Thus, if a H atom binds on an empty dimer, there is a loss of the π-bond stabilization, whereas if it binds on a half-filled dimer, there is no increase in the total energy. Estimates of the π-bond stabilization range from a few kcal/mol[14,15] based on the modeling of the thermal desorption kinetics to 18 kcal/mol based on the STM results.[16] The effect is not limited to the interaction of hydrogen with Si(100). STM measurements have suggested that O_2 preferentially dissociatively chemisorbs at the unoccupied sites of half-filled dimers on hydrogen terminated Si(100)[17] and that Cl_2 preferentially dissociatively chemisorbs onto the adjacent sites within a single empty dimer on Si(100).[18]

The enhanced reactivity of an unoccupied site in a half-filled dimer relative to that in an empty dimer for adsorption of the complementary F atom observed in the present study is in contrast to the predictions of a molecular dynamics simulation to describe the interaction of F_2 with Si(100). The simulation results suggest that two atom adsorption occurs preferentially, although not exclusively, across adjacent dimer rows[12] as opposed to on the same dimer. This contradiction with experiment, along with that regarding the relative probabilities of single atom and two atom adsorption, indicates that the currently available potential[12] is an inaccurate representation of the interaction between F_2 and Si.

c. Molecular steering. Recently there have been many experimental[19,20] and theoretical[21–23] investigations of a phenomenon termed molecular steering in which the incident molecule is oriented by the gas–surface interaction potential along a more favorable trajectory to reaction than expected from a random orientation. This effect is expected to be accentuated in experiments employing supersonic molecular beams because the extreme rotational cooling ($T_{rot} \sim 5$ K) of the molecules in the beam makes them more susceptible to rotation by an external force, such as the gas–surface interaction potential. The large value for the cross section for F atom abstraction from F_2 incident on Si(100), $B = 24.7 \times 10^{-16}$ cm^2, relative to the cross-sectional area of a surface site, 14.7×10^{-16} cm^2, suggests the presence of an attractive gas–surface interaction potential that is consistent with the notion of molecular steering in the interaction of F_2 with Si(100).

B. Limitations of model

Although the four-site model offers a good description of the kinetics of the interaction of F_2 with Si(100) as well as a physically intuitive picture of this gas–surface interaction, a few assumptions were made in its development that warrant further discussion.

One of the limitations of the model is that the saturation coverage of F on Si is defined to be 1 ML, the number of dangling bonds on the Si(100) surface. While the experimental results show that the saturation coverage is indeed about 1 ML, the measured value, 0.94 ± 0.11 ML, falls just short. However, the uncertainty in the experimental measurement does not preclude the value from being 1 ML. The largest source of error is the literature value for the electron bombardment ionization cross section of the F atom, which has an uncertainty of 20%. Because the probability of single atom abstraction (P_1) is directly proportional to it and the probability of two atom adsorption (P_2) is directly related to P_1, the experimentally determined saturation coverage does increase to 1 ML upon increasing the value of the ionization cross section by 20%. On the other hand, it is possible that the saturation coverage is slightly lower than 1 ML because of defects on the surface that might eliminate dimer atoms, and hence eliminate dangling bonds, leading to a decrease in the total number of available adsorption sites. Scanning tunneling microscope images of clean Si(100) surfaces have shown defect densities on the order of a few percent.[24] While the model could have been modified by redefining the saturation coverage, θ_{sat}, to be less than 1 ML, this modification would have created an additional variable, θ_{sat} for which there is no clear justification.

Regardless of the absolute value of θ_{sat}, the values of P_1 and P_2 decay towards zero as the coverage approaches θ_{sat} far more rapidly than predicted by the model. This effect is probably a result of the last remaining unoccupied dangling bonds being less accessible due to steric hindrance than expected according to simple statistics or much less reactive because of the effects of neighboring adsorbates. The absence of any effect from neighboring adsorbates other than the complementary surface atom of the dimer pair is another significant limitation of the model. The effect of neighboring adsorbates could be incorporated into the model by incorporating a coverage dependence into the cross sections and X. Although this modification certainly would have been a more accurate description of reality, the additional complexity would diminish the physical insight gained from the simplicity of the model.

The model also assumes that X, the fraction of complementary F atoms that scatter directly into the gas phase, is independent of the type of site on which the initial abstraction occurs. This assumption implies that the dynamics of the direct scattering of the F atom after an abstraction event on a dangling bond of a half-filled dimer are not significantly different from that of an empty dimer. It is justified by the independence of the angular and velocity distributions of the

scattered F atom on coverage,[1] because the relative numbers of unoccupied sites on a half-filled and on an empty dimer vary significantly with coverage.

Finally, the statistical basis of the model is founded on the assumption that adsorption sites are accessed randomly by the incident F_2 molecules and that there is no diffusion or desorption of an adsorbed F atom once it is bound to a dangling bond site. The diffusion constraint eliminates any inhomogeneity in the spatial distribution of adsorbates that might arise from their islanding, allowing the global coverage to be truly representative of the local adsorbate density in the vicinity of the random site of the interaction. This simplifying assumption is justified by STM images of Si(111) at low fluorine coverage[11] which show random fluorine adsorption sites with no significant islanding or clustering of adsorbates. In addition, repeated imaging of the fluorinated surface shows no significant adsorbate motion, through either diffusion or desorption. Both constraints are additionally justified by the high bond strength of the Si–F bond, 150 kcal/mol,[25,26] relative to the diffusion and desorption barriers. In general, adsorbate diffusion barriers are on the order of 5%–20% of the surface–adsorbate bond strength[27] and desorption barriers are at least equivalent to the surface–adsorbate bond strength, making both barriers in this system much greater than kT. In addition, the depletion of adsorbed F atoms by desorption of a fluorosilane etch product is not observed to occur in the interaction of low energy F_2 with Si(100) at 250 K.[1]

The model is also based on the assumption that there is no diffusion of F_2 as a molecularly adsorbed precursor, either extrinsic or intrinsic, prior to reaction. This assumption is justified by lack of experimental evidence for a precursor molecule. Specifically, the strong dependence of the unreactive scattering probability, P_0, on coverage precludes the existence of an extrinsic precursor while the lack of a dependence of the F_2 scattering and reaction dynamics on the incident energy below 1.5 kcal/mol indicates the absence of an intrinsic precursor. Sholl[28] has examined the effect of a physisorbed precursor mechanism using Monte Carlo simulations that incorporate a model similar to the two-site model described above in Sec. IV A 5 a. A comparison of these simulations with the experimental results shown in Fig. 1 suggests that a precursor mechanism has no significant, if any, contributions to the kinetics of the interaction of F_2 with Si.

V. CONCLUSIONS

Molecular fluorine interacts with Si(100) via a novel dissociative chemisorption mechanism called atom abstraction and results in two reactive channels, single atom abstraction and two atom adsorption in which one and two F atoms adsorb to the surface, respectively. The distinguishing feature of single atom abstraction and two atom adsorption from classic dissociative chemisorption is that only one surface–adsorbate bond is necessary to liberate sufficient energy to cleave the incident molecular bond. As a consequence, the fate of the complementary F atom is not necessarily as an adsorbate on the surface as it is in classic dissociative chemisorption in which the two fragments of the cleaved molecule adsorb to the surface in a concerted process. The complementary F atom may scatter into the gas phase leading to single atom abstraction, or it may subsequently interact with the surface and adsorb leading to two atom adsorption.

The kinetics of the interaction of F_2 with Si(100)(2×1) cannot be described by traditional gas–surface kinetics models. Instead, a statistical model is able to describe the kinetics of single atom abstraction and two atom adsorption that is based on the premise that single atom abstraction and two atom adsorption share a common initial step, F atom abstraction, and that the four distinct types of sites, sites on empty dimers and filled dimers as well as unoccupied and occupied sites on half-filled dimers, interact differently with the incident F_2 molecule and scattered F atom. The model describes the data well, and the results are consistent with a stepwise mechanism in which the initial atom abstraction is central to both single atom abstraction and two atom adsorption. This result is expected since there is no thermodynamic driving force requiring the adsorption of the second F atom. The results of the model suggest that the fate of the complementary F atom is determined, in part, by the orientation of the incident F_2 molecular axis with respect to the surface. If the molecular axis of the incident F_2 is oriented within 30° of the surface normal, the complementary F atom will likely be ejected away from the surface making two atom adsorption impossible. This mechanism is termed ''neighbor-independent'' because the fate of the complementary F atom is independent of the occupancy of the other sites on the surface. At zero coverage, it is this mechanism that yields the nonzero probability for single atom abstraction. On the other hand, if the F_2 molecular axis is oriented more than 30° from the surface normal, the complementary F atom will likely interact with the surface. If the F atom interacts with an unoccupied site, adsorption may occur. This mechanism is termed ''neighbor-dependent'' because the occupancy of the site with which the F atom interacts determines whether the overall result is single atom abstraction or two atom adsorption. It is the competition between the need for an unoccupied site for the initial atom abstraction, and the subsequent need for an occupied site to prevent adsorption of the complementary F atom that yields the unusual coverage dependence of the probability of single atom abstraction which is signified by a maximum likelihood at about 0.5 ML coverage.

The results of the model also show that the unoccupied sites on half-filled dimers are about twice as reactive as the unoccupied sites on empty dimers. The cross section for F atom abstraction by an unoccupied dangling bond on a half-filled dimer is $24.7\times10^{-16}\,\mathrm{cm}^2$ while that on an empty dimer is $14.0\times10^{-16}\,\mathrm{cm}^2$. This result is consistent with a lower stability of the unoccupied dangling bond in a half-filled dimer because of the absence of the π interaction that exists between the two unoccupied dangling bonds in an empty dimer and, therefore, a higher reactivity. The necessity for differentiation of the reactivity of the distinct surface sites is demonstrated by the poor ability of the model to describe the data when there is no differentiation of sites. Finally, the total reaction probability is near unity at zero coverage which indicates that there is no barrier to reaction.

The results of the model suggest that the unoccupied sites on the half-filled dimer are so reactive that they are able to attract the incident F_2 molecule from a distance extending beyond the cross sectional area of the site itself. These results likely reflect the phenomenon of molecular steering in which the incident molecules are aligned into a favorable orientation for reaction.

Atom abstraction is not unique to the interaction of F_2 with Si(100). Atom abstraction ought to be present in any gas–surface system in which the energy liberated by the formation of a single surface–adsorbate bond is sufficient to cleave the incident molecular bond. Although no previous experimental investigation has provided direct evidence of atom abstraction, several investigations have provided experimental evidence that is consistent with the presence of atom abstraction.[11,29–32] Despite the dearth of experimental evidence demonstrating atom abstraction, this gas-surface mechanism may have significant implications in important chemical processes like heterogeneous catalysis, chemical vapor deposition, and semiconductor etching. The possibility of atom abstraction ought to be considered in reaction systems in which atom abstraction is energetically favorable, especially in situations in which the production of radical atoms and molecules may have a significant effect on the rest of the system.

ACKNOWLEDGMENTS

M.R.T. acknowledges the support of DOD through a NDSEG-ONR Predoctoral Fellowship and J. R. Holt for assistance with numerical analysis. This work is supported by NSF CHE-9713276.

[1] M. R. Tate, D. Gosalvez-Blanco, D. P. Pullman, A. A. Tsekouras, Y. L. Li, J. J. Yang, K. B. Laughlin, S. C. Eckman, M. F. Bertino, and S. T. Ceyer, J. Chem. Phys. **111**, 3679 (1999).
[2] Y. L. Li, D. P. Pullman, J. J. Yang, A. A. Tsekouras, D. B. Gosalvez, K. B. Laughlin, Z. Zhang, M. T. Schulberg, D. J. Gladstone, and S. T. Ceyer, Phys. Rev. Lett. **74**, 2603 (1995).
[3] S. T. Ceyer, *Proc. R. A. Welch Found. Conf. Chem. Res. XXXVIII: Chemical Dynamics of Transient Species* (Welch Foundation, Houston, 1994), pp. 156–172; D. P. Pullman and S. T. Ceyer, Abstracts of the ACS **207**, 168 (1994).
[4] S. T. Ceyer, D. J. Gladstone, M. McGonigal, and M. T. Schulberg, *Physical Methods of Chemistry*, edited by B. W. Rossiter and R. C. Baetzold (Wiley, New York, 1993), 2nd ed., Vol. IXA, p. 383.
[5] J. J. Yang, Ph.D. Thesis, Massachusetts Institute of Technology, 1993.
[6] D. Gosalvez-Blanco, Ph.D. Thesis, Massachusetts Institute of Technology, 1997.
[7] M. R. Tate, Ph.D. Thesis, Massachusetts Institute of Technology, 1999.
[8] T. R. Hayes, R. C. Wetzel, and R. S. Freund, Phys. Rev. A **35**, 578 (1987).
[9] P. R. Bevington and D. K. Robinson, *Data Reduction and Error Analysis for the Physical Sciences*, 2nd ed. (McGraw-Hill, New York, 1992), p. 195.
[10] J. O. Hirschfelder, C. F. Curtiss, and R. B. Bird, *Molecular Theory of Gases and Liquids* (Wiley, New York, 1964), p. 1111.
[11] J. A. Jensen, C. Yan, and A. C. Kummel, Science **267**, 493 (1995).
[12] L. E. Carter, S. Khodabandeh, P. C. Weakliem, and E. A. Carter, J. Chem. Phys. **100**, 2277 (1994).
[13] J. A. Appelbaum, G. A. Baraff, and D. R. Hamann, Phys. Rev. B **14**, 588 (1976).
[14] M. C. Flowers, N. B. H. Jonathan, A. Morris, and S. Wright, J. Chem. Phys. **108**, 3342 (1998).
[15] M. P. D'Evelyn, Y. L. Yang, and L. F. Sutcu, J. Chem. Phys. **96**, 852 (1991).
[16] J. J. Boland, Phys. Rev. Lett. **67**, 1539 (1991).
[17] H. Kajiyama, S. Heike, T. Hitosugi, and T. Hashizume, Jpn. J. Appl. Phys., Part 2 **37**, L1350 (1998).
[18] I. Lyubinetsky, Z. Dohnálek, W. J. Choyke, and J. T. Yates, Phys. Rev. B **58**, 7950 (1998).
[19] M. Beutl, M. Riedler, and K. D. Rendulic, Chem. Phys. Lett. **247**, 249 (1995).
[20] M. Gostein and G. O. Sitz, J. Chem. Phys. **106**, 7378 (1997).
[21] A. Gross, S. Wilke, and M. Scheffler, Phys. Rev. Lett. **75**, 2718 (1995).
[22] M. Kay, G. R. Darling, S. Holloway, J. A. White, and D. M. Bird, Chem. Phys. Lett. **245**, 311 (1995).
[23] G. R. Darling, M. Kay, and S. Holloway, Surf. Sci. **400**, 314 (1998).
[24] J. J. Boland, Adv. Phys. **42**, 129 (1993).
[25] R. Walsh, Acc. Chem. Res. **14**, 246 (1981).
[26] C. J. Wu and E. A. Carter, J. Am. Chem. Soc. **113**, 9061 (1991).
[27] A. Zangwill, *Physics at Surfaces* (Cambridge University Press, Cambridge, 1988), p. 379.
[28] D. S. Sholl, J. Chem. Phys. **106**, 289 (1997).
[29] D. J. Driscoll, W. Martir, J. X. Wang, and J. H. Lunsford, J. Am. Chem. Soc. **107**, 58 (1985).
[30] X. L. Zhou, S. R. Coon, and J. M. White, J. Chem. Phys. **94**, 1613 (1991).
[31] J. L. Lin and B. E. Bent, J. Am. Chem. Soc. **115**, 2849 (1993).
[32] J. Strömquist, L. Hellberg, B. Kasemo, and B. I. Lundqvist, Surf. Sci. **352**, 435 (1996).